forests

MDPI

Article

Study on the Mechanical Properties and Basic Elastic Constants of Yunnan *Dendrocalamus sinicus Chia et J. L. Sun*

Fengwei Zhou, Xingyu Wang, Yanrong Wang, Guofu Li and Chunlei Dong *

College of Materials and Chemical Engineering, Southwest Forestry University, Kunming 650224, China; fengweizhou@swfu.edu.cn (F.Z.); wangxingyu@swfu.edu.cn (X.W.); wyanrong@swfu.edu.cn (Y.W.); lgf183@swfu.edu.cn (G.L.)
* Correspondence: dchunlei@swfu.edu.cn

Abstract: Yunnan *Dendrocalamus sinicus Chia et J. L. Sun* (YDS) is a giant bamboo species with a diameter at breast height of up to nearly 40 cm. It is endemic to Yunnan, China, and only a very small portion of it is directly used as load-bearing beams and columns in the dwellings of ethnic minorities, such as in Dai architecture. Due to the structural characteristics of its hollow and thin walls, systematic physical and mechanical property testing of this species faces significant challenges in terms of methods and means. This issue has become one of the main barriers to the realization of its large-scale industrial use. Therefore, this paper systematically tests and studies YDS's three kinds of strength (tension, compression, and shear), modulus of elasticity, and six Poisson's ratios with the help of digital image correlation (DIC) technology and self-created material testing methods. The (1) tensile, compressive, and shear strengths and moduli in longitudinal, radial, and chordal directions; (2) tensile strengths and moduli of bamboo green, flesh, and yellow layers in the thickness direction of the bamboo wall; and (3) six Poisson's ratios under tensile and compressive stresses were obtained for YDS. It was also found that the tensile strength (378.8 MPa) of the green layer of YDS exceeded the yield strength (355 MPa) of 45# steel, making it a potential high-strength engineering material or fiber-reinforced material.

Keywords: Yunnan *Dendrocalamus sinicus Chia et J. L. Sun*; constant of elasticity; poisson's ratio; digital image correlation

Citation: Zhou, F.; Wang, X.; Wang, Y.; Li, G.; Dong, C. Study on the Mechanical Properties and Basic Elastic Constants of Yunnan *Dendrocalamus sinicus Chia et J. L. Sun*. *Forests* **2024**, *15*, 2017. https://doi.org/10.3390/f15112017

Received: 11 October 2024
Revised: 24 October 2024
Accepted: 5 November 2024
Published: 15 November 2024

1. Introduction

Yunnan *Dendrocalamus sinicus Chia et J. L. Sun*, a bamboo species endemic to Yunnan, China, is characterized by its large culm diameter and rapid growth rate [1]. It possesses high density, hardness, and strength [2,3], which leads to its frequent use as load-bearing beams and columns in many traditional ethnic minority architectures, such as the residential buildings of the Dai people in Yunnan and the Miao people in Guizhou [4]. However, similar to other bamboo materials, the industrial processing and utilization of YDS in its raw form are relatively limited. Currently, the academic and industrial sectors primarily employ conventional wood-based panel manufacturing philosophies and methods for the development and utilization of bamboo. This involves the disassembly of the raw material into smaller units, which are then reassembled into various types of wood-based panels, such as bamboo-wood composite flooring [5], bamboo laminated veneer lumber [6], bamboo particleboard [7], and reconstituted bamboo [8]. This processing method results in significant destruction of the original bamboo form, leading to low material utilization rates and complex, energy-intensive manufacturing processes. Additionally, the current research on the mechanical properties of bamboo materials by many scholars is relatively singular, lacking systematic and in-depth studies. Therefore, to enhance the efficient use of raw bamboo in the fields of construction and materials, and to reduce energy consumption in processing and utilization, it is crucial to investigate the mechanical properties of bamboo with radial gradient variations from the bamboo's outer

layer to the inner layer, as well as the related elastic constants and the strain conditions of bamboo under different stress states.

Previous studies on the physical and mechanical properties of bamboo have predominantly focused on the individual mechanical performance of bamboo fiber bundles, entire bamboo poles, and small-sized bamboo specimens, such as longitudinal tensile and compressive properties. For example, Wang et al. investigated the tensile properties and fracture modes of the fiber bundles of *Phyllostachys edulis*, and their results showed that the strength and modulus of the bamboo fibers increase progressively from the inner part to the outer part [9]. The strength and elastic modulus of bamboo are positively correlated with density and fiber volume fraction [10–12]. This indicates that bamboo fibers are the primary load-bearing structures within the bamboo, with an elastic modulus significantly higher than that of the matrix tissue. The matrix tissue effectively absorbs, transmits, and distributes loads evenly, which contributes to the overall strength of the bamboo being greater than that of a single fiber bundle [13]. Yang utilized Digital Image Correlation (DIC) and resistive strain gauge testing methods to investigate the longitudinal tensile properties of Moso bamboo from the inner to the outer layers. The results indicated that due to the higher proportion of fiber bundles in the outer layer of the bamboo wall, the tensile properties of the outer layer are significantly higher than those of the inner layer [14]. Sharma determined the radial tensile and compressive mechanical properties of the culms of bamboo, and the findings demonstrated that the culms exhibit brittle failure under low stress levels in both radial tension and compression, with the thickness of the bamboo wall being positively correlated with the radial strength and modulus of the culms [15]. Davies, Zhou, and Liu et al., respectively conducted studies on the longitudinal, radial, and tangential tensile and compressive properties of Moso bamboo and bamboo composite materials. Their outcomes consistently showed that the longitudinal mechanical properties of bamboo are significantly superior to the radial and tangential properties, and there is a strong correlation between the mechanical properties of bamboo and its density [16–18].

Elastic constants are fundamental material parameters for the numerical modeling of bamboo and bamboo-wood composites [19,20]. However, compared to the study of common physical and mechanical properties of bamboo, research on the elastic constants, particularly the Poisson's ratio of bamboo, is relatively scarce. This has become a significant factor limiting the innovative use of bamboo in the field of new material research. In existing studies, research on the six common Poisson's ratios, three elastic moduli, and three shear moduli is not comprehensive, with most studies focusing only on one aspect, lacking systematic research. Molari used DIC technology to investigate the longitudinal tensile and compressive properties of bamboo, and the results showed that the longitudinal tensile modulus of bamboo is about three times its compressive modulus, with longitudinal tensile and compressive Poisson's ratios of 0.47 and 0.56, respectively [21]. Lu found that the Poisson's ratio of Moso bamboo is positively correlated with its density, cellulose content, and the angle of microfibers, and the Poisson's ratio decreases from the bamboo's outer layer to the inner layer [22]. García determined the radial-hoop Poisson's ratio, hoop Young's modulus, and hoop-longitudinal shear modulus of bamboo using ring-shaped specimens, and the results indicated that the radial-hoop Poisson's ratios at the bottom, middle, and top of the bamboo culm are 0.43, 0.14, and 0.12, respectively; the hoop Young's modulus is 398 MPa; and the hoop-longitudinal shear modulus is 581 MPa [23].

The transverse section of bamboo exhibits a naturally cylindrical structure with thin walls and a gradual distribution of bamboo fiber bundles along the wall thickness direction [24]. These factors lead to numerous challenges and difficulties in the preparation methods for specimens in the longitudinal, radial, and tangential directions, as well as in the basic mechanical property testing techniques. This also accounts for the reason why most previous studies on the fundamental mechanical properties of bamboo have not been comprehensive and systematic in terms of parameter testing.

To address this, the present study aims to employ a digital speckle interferometer and innovative material testing methods to systematically investigate the longitudinal tensile

strength, modulus, and Poisson's ratio of the bamboo's outer layer, middle layer, and inner layer of YDS. Additionally, the study will examine the longitudinal, radial, and tangential strength, modulus, and Poisson's ratio of the bamboo wall layers under tensile, compressive, and shear load conditions. Concurrently, the research will conduct a systematic investigation of the stress and strain in different positions of the bamboo under various loading states. This approach will yield a comprehensive set of fundamental mechanical properties and elastic constants for YDS, providing foundational support for the utilization of its significant potential in high-strength construction materials and composite fields.

2. Materials and Methods

The raw bamboo of YDS is harvested from the Lincang area of Yunnan Province. Its cross-section possesses a naturally cylindrical structure with relatively large wall thickness, and the bamboo fiber bundles exhibit a radial gradient distribution from the outer layer to the inner layer, as depicted in Figure 1a. After undergoing natural air-drying treatment, the root and tip portions are removed to obtain internodal segments approximately 3 m in length. Subsequently, by eliminating the bamboo nodes, culms of about 400 mm in length, with an outer diameter of around 115 mm and a wall thickness of about 15 mm, are acquired.

In accordance with the standards set forth in D07 Committee, "Standard Test Methods for Small Clear Specimens of Timber" [25] and JG/T199-2007, "Test Methods for Physical and Mechanical Properties of Bamboo for Construction" [26], in accordance with the three mechanical property test types (tension, compression, and shear), the bamboo tube was divided into bamboo boards with a width of approximately 25 mm. The surface layer of bamboo, which was green and yellow in color, was partially shaved off, and the test specimens were prepared in accordance with the sampling and specimen preparation methods illustrated in Figure 1b. The initial letter in the specimen designation represents the mode of loading applied to the bamboo material. Thus, "T" corresponds to tension, "C" to compression, and "S" to shear. The second letter indicates the sample location, with "I" denoting the inner layer's yellow region of the bamboo wall, "O" denoting the outer layer's green region of the bamboo wall, and "M" denoting the pith region of the middle layer. The third letter denotes the defined orientation of the bamboo, specifically "L" for longitudinal, "R" for radial, and "T" for tangential directions.

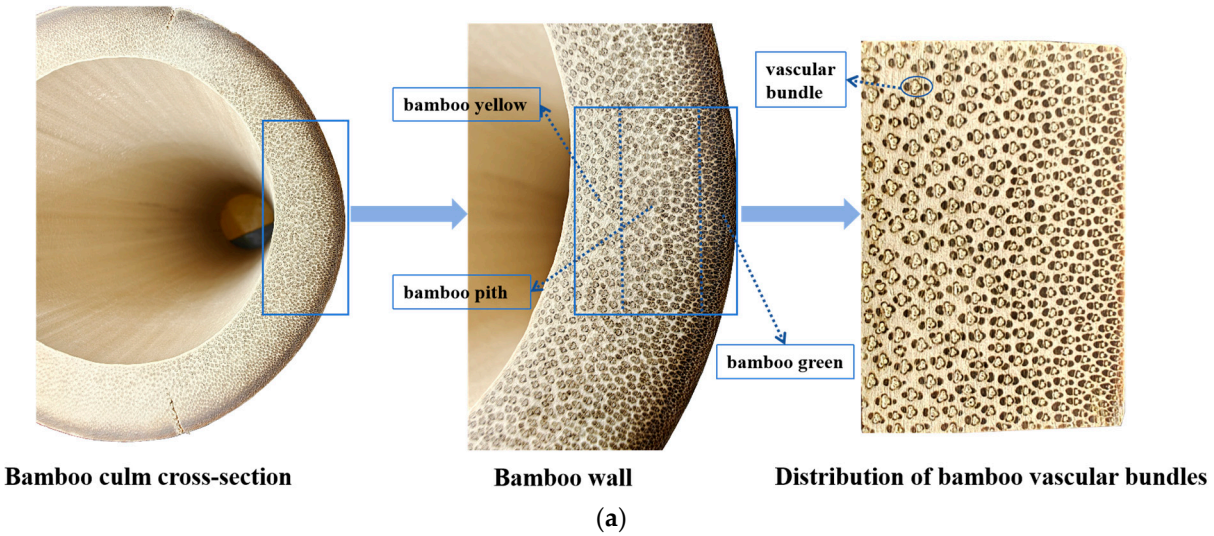

Figure 1. *Cont.*

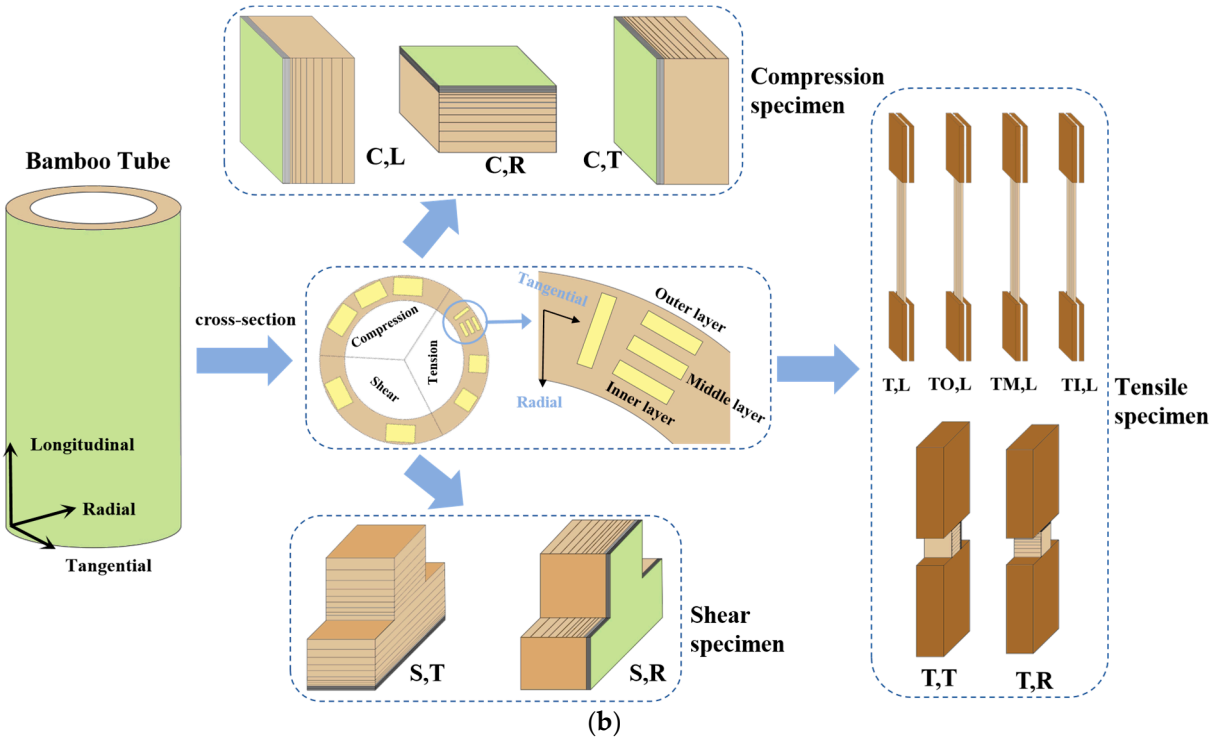

Figure 1. Schematic diagram of bamboo cross-section and sample preparation: (**a**) Distribution of vascular bundles in the bamboo cross-section, (**b**) Schematic diagram of sample extraction and preparation.

It is important to note that when fabricating longitudinal tensile specimens, consideration must be given to the thicker walls of YDS and the fact that the density of the green outer layer of the bamboo is significantly higher than that of the yellow inner layer. Accordingly, four distinct types of longitudinal tensile specimens were fabricated for the experimental investigation: specifically, the outer green portion of the bamboo wall, the middle flesh portion of the bamboo, the inner yellow portion of the bamboo wall, and a composite bamboo wall layer incorporating the green, flesh, and yellow portions of the bamboo. In order to conduct mechanical tests on the radial and tangential tensile specimens, two Yunnan pine blocks with identical cross-sectional dimensions were affixed at either end of the radial and chordal directions as the clamping ends. The tensile, compression and shear specimens of YDS are illustrated in Figure 2.

Once all specimens had been prepared, they were equilibrated for a period of two weeks in a Binder climatic chamber (The model is Binder MKF720, manufactured by BINDER GmbH in Tuttingen, Germany) at a temperature of 20 ± 0.1 °C and a relative humidity of 65 ± 2%. Following the aforementioned equilibration period, the mechanical properties of the bamboo were evaluated using a Shimadzu Mechanical Testing Machine (The model is AGS-X-100KN, with a precision of 1N, and is manufactured by Shimadzu Corporation in Kyoto, Japan) and LINCONST DIC. The digital speckle interferometer LINCONST DIC system, developed and manufactured by Lian Heng Optics (Suzhou, China) Intelligent Technology Co., Ltd., is equipped with the LVE video extensometer system as its analytical software (The version is LVE PRO V24.10.60). The underlying principle of this system is based on digital camera technology and image processing algorithms that capture and analyze the changes in the image features of a specimen during the loading process, enabling real-time measurement of its displacement and strain. The operational procedure involves the initiation of loading by the mechanical testing machine, prompting the digital speckle interferometer to conduct real-time imaging of the specimen that has been sprayed with a speckle pattern. Concurrently, the LVE analysis software is used to delineate measurement domains within the captured images, establish seed points, and analyze the longitudinal and transverse displacements of the speckles as the specimen is subjected to force. By cor-

relating the force values with the displacement data, the system can analyze and calculate the full-field stress, strain, elastic modulus, and Poisson's ratio of the specimen throughout the loading process.

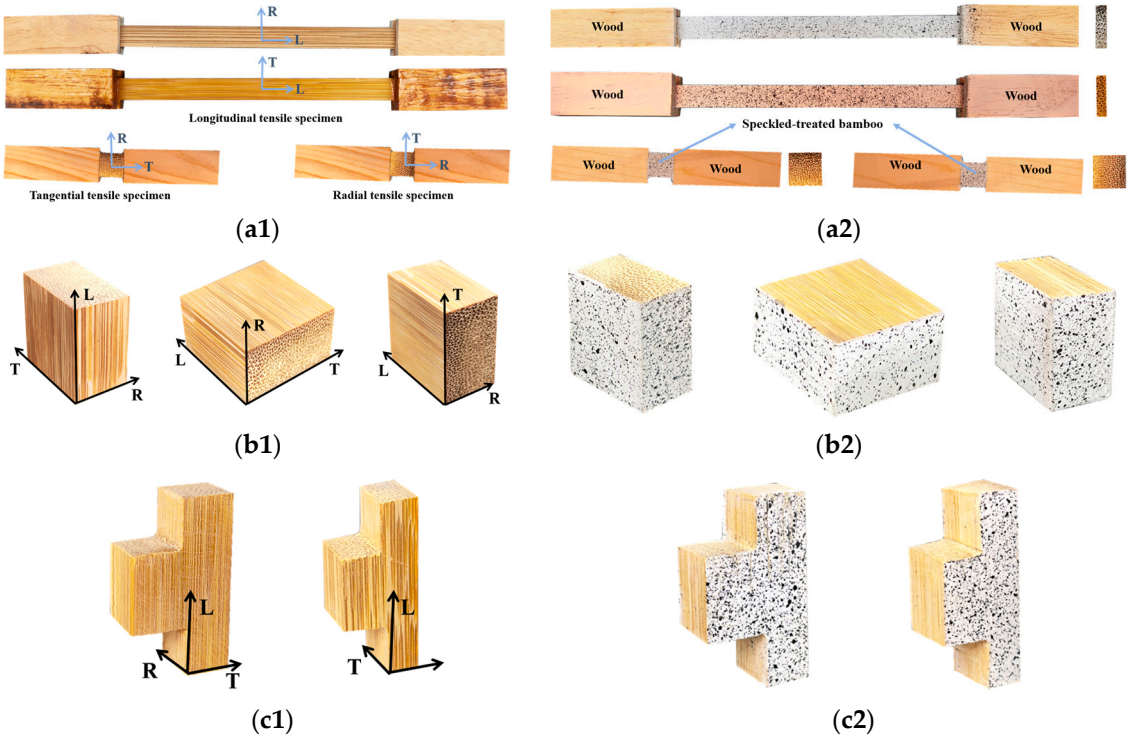

Figure 2. Basic mechanical properties of YDS test specimens: (**a1**) longitudinal, radial and chordal tensile specimens, (**b1**) longitudinal, radial and chordal compression specimens, and (**c1**) radial and chordal shear specimens, of which (**a2–c2**) each represent the corresponding test specimens after undergoing surface spray speckle treatment.

The tests are all destructive and the specimen modulus and corresponding Poisson's ratio are calculated during the elastic phase, so that a single specimen represents a repeated test in the various mechanical property tests. The type, number of samples, specimen size, and density in terms of moisture content of the bamboo, as well as the symbols for each mechanical strength and elasticity constant of the bamboo tested for each mechanical property, are listed in Table 1.

Table 1. List of mechanical property tests of YDS.

Test Types	Specimens Naming	Specimen Quantities	Specimens Size: L × R × T (mm)	Densities (g/cm^3)	Moisture Contents (%)	Loading Speeds (mm/min)	Strength	Elasticity/Shear Modulus	Poisson's Ratios
Tension	TI, L	8	130.20 × 2.53 × 10.04	0.523	9.35	1	$f_{TI,L}$	$E_{TI,L}$	$\mu_{LTI(T)}$
	TM, L	8	130.22 × 2.55 × 10.12	0.648	9.29	1	$f_{TM,L}$	$E_{TM,L}$	$\mu_{LTM(T)}$
	TO, L	8	130.10 × 2.51 × 10.05	0.811	9.21	1	f_{TOL}	$E_{TO,L}$	$\mu_{LTO(T)}$
	T, L	8	130.26 × 2.53 × 10.14	0.657	9.35	1	$f_{T,L}$	$E_{T,L}$	$\mu_{LR(T)}$
	T, R	24	12.09 × 12.06 × 12.04	0.643	9.30	0.5	$f_{T,R}$	$E_{T,R}$	$\mu_{RL(T)}$, $\mu_{RT(T)}$
	T, T	24	12.09 × 12.08 × 12.03	0.653	9.22	0.5	$f_{T,T}$	$E_{T,T}$	$\mu_{TL(T)}$, $\mu_{TR(T)}$
Compression	C, L	36	21.05 × 12.05 × 20.04	0.646	9.14	0.7	$f_{C,L}$	$E_{C,L}$	$\mu_{LTI(C)}$, $\mu_{LTO(C)}$, $\mu_{LTI(C)}$
	C, R	24	21.04 × 12.04 × 20.03	0.641	9.32	0.5	$f_{C,R}$	$E_{C,R}$	$\mu_{RL(C)}$, $\mu_{RT(C)}$
	C, T	36	21.06 × 12.05 × 20.07	0.649	9.17	0.5	$f_{C,T}$	$E_{C,T}$	$\mu_{TLI(C)}$, $\mu_{TLQ(C)}$, $\mu_{TR(C)}$
Shear	S, R	8	Shear surface: 15.51 × 12.05	0.647	9.48	0.3	$f_{S,R}$	G_R	-
	S, T	8	shear surface: 15.52 × 12.06	0.644	9.28	0.3	$f_{S,T}$	G_T	-

3. Results and Discussion

3.1. Load-Displacement Curves and Failure Modes

3.1.1. Tension

Figure 3a–f displays the load-displacement curves for all tensile test specimens of YDS. By using the "Calculate the average of multiple curves" function in Origin software (The version is Origin 2024) on the six curves from each mechanical test type, the average load-displacement curve for the tensile tests of YDS can be obtained, as shown by the red line in Figure 3. Subsequent discussions in the text regarding the compression and shear load-displacement curves are represented in the same manner.

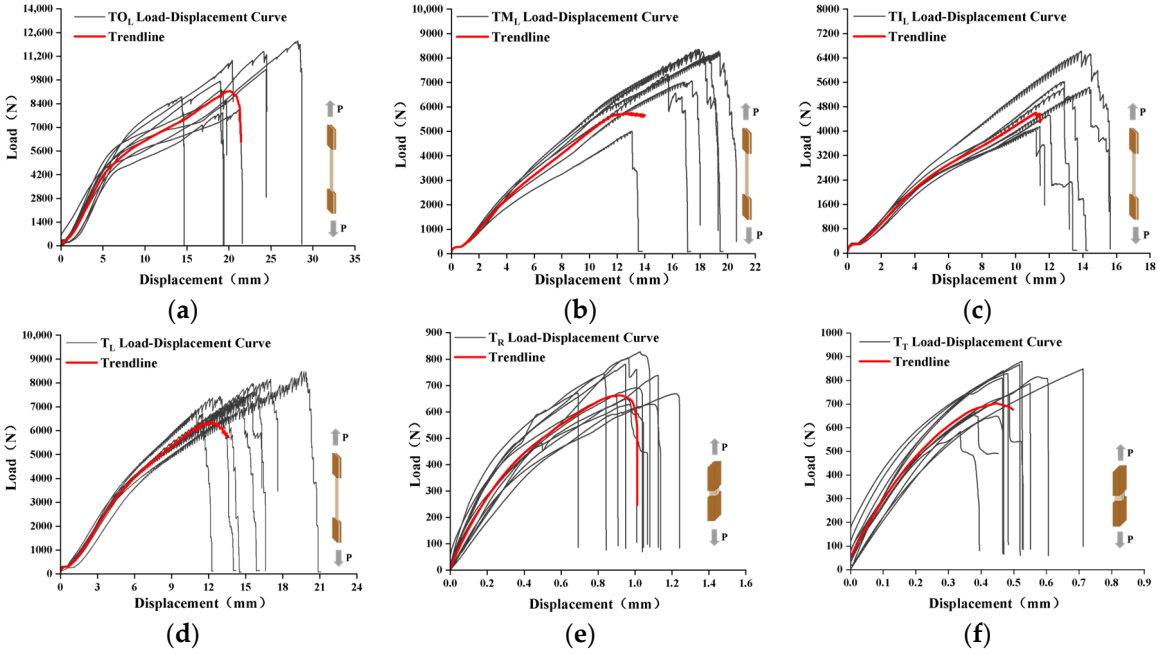

Figure 3. YDS tensile load-displacement curves: (**a**) longitudinal tension of bamboo green layer, (**b**) longitudinal tension of bamboo flesh layer, (**c**) longitudinal tension of bamboo yellow layer, (**d**) longitudinal tension containing bamboo green and flesh and bamboo yellow, (**e**) radial tension, (**f**) tangential tension.

The load-displacement curves of the bamboo green layer, the bamboo flesh layer, the bamboo yellow layer, and the bamboo wall layer, which contains the bamboo green and flesh layers and the bamboo yellow layer, exhibited similarities in the longitudinal tensile tests of YDS. Similar to previous research findings, these curves could be classified into the four phases of linear elasticity, reinforcement, plasticity, and brittle damage [27]. Additionally, it was observed that there was notable elastic behavior and brittle damage. From the data presented in Figure 3a–d, it can be observed that the average destructive load of the bamboo green layer (7850 N) is the highest, followed by the average destructive load of the bamboo flesh layer (7401 N) and the average destructive load of the bamboo yellow layer, which contains both the bamboo green and flesh layers (7564 N). In contrast, the average destructive load of the bamboo flesh layer (5125 N) is the lowest. As illustrated in Figure 3e, f, the tensile load-displacement curves of YDS in the radial and tangential directions exhibit a similar pattern, comprising three stages: linear elasticity, plasticity, and brittle failure. The tensile performance is notably inferior, with an average destructive load of approximately 700 N.

This is because bamboo is a natural composite material composed of vascular bundles and basic tissue, and the density of the vascular bundles in bamboo gradually increases from the inner bamboo to the outer bamboo. Therefore, in terms of material science, bamboo is actually a non-uniform anisotropic material [28], which results in significant

differences in its mechanical properties in different directions. Compared to conventional commercial timber, this gradually changing composite structure endows bamboo with extremely strong physical and mechanical properties in the longitudinal direction [29]. However, the bamboo fibers in the radial and tangential directions are arranged parallel to each other, and the part that bears the external load is mainly the bamboo matrix, leading to the poorest tensile properties in these two directions.

YDS exhibits reinforcement phenomena during the longitudinal tensile process, which is attributed to its characteristics as a natural fiber-reinforced composite material. The bamboo fiber bundles within the material possess excellent tensile properties and are aligned along the longitudinal direction, coinciding with the direction of longitudinal stress [30]. Consequently, the bamboo fiber bundles can be likened to the "reinforcing bars" in reinforced concrete, while the bamboo matrix can be considered as the "concrete". The inter-support between the fiber bundles and the matrix allows the bamboo material to collectively withstand greater external loads in the longitudinal direction.

Figure 4 illustrates the typical tensile damage schematic of YDS, and the ultimate strain map obtained from the analysis of DIC data in the vicinity of the damage event. In the longitudinal tensile test, only the typical tensile damage schematic of the bamboo green layer and the ultimate strain map are presented, as the damage modes and types of the bamboo green layer, bamboo flesh layer, bamboo yellow layer, and all samples containing these layers are found to be highly similar. During the testing process, when the ultimate load is reached, the bamboo fiber bundles at the edge of the bamboo material gradually break with accompanying faint sounds, ultimately leading to brittle failure with a sharp crack. This is different from the findings of other researchers [31,32], where the bamboo does not fail by breaking in the weaker areas but rather "explodes" into numerous fine bamboo bundles, as shown in Figure 4a. Radial and tangential tensile tests both result in brittle failure without any obvious precursors to damage. The radial tensile damage is predominantly observed in the vicinity of the bamboo yellow region, as illustrated in Figure 4b. The tangential tensile damage was initially caused by the formation of cracks in the region proximate to the bamboo yellow. With the increase in load, the cracks gradually extended from the bamboo yellow to the bamboo green region, resulting in the observed damage, as illustrated in Figure 4c.

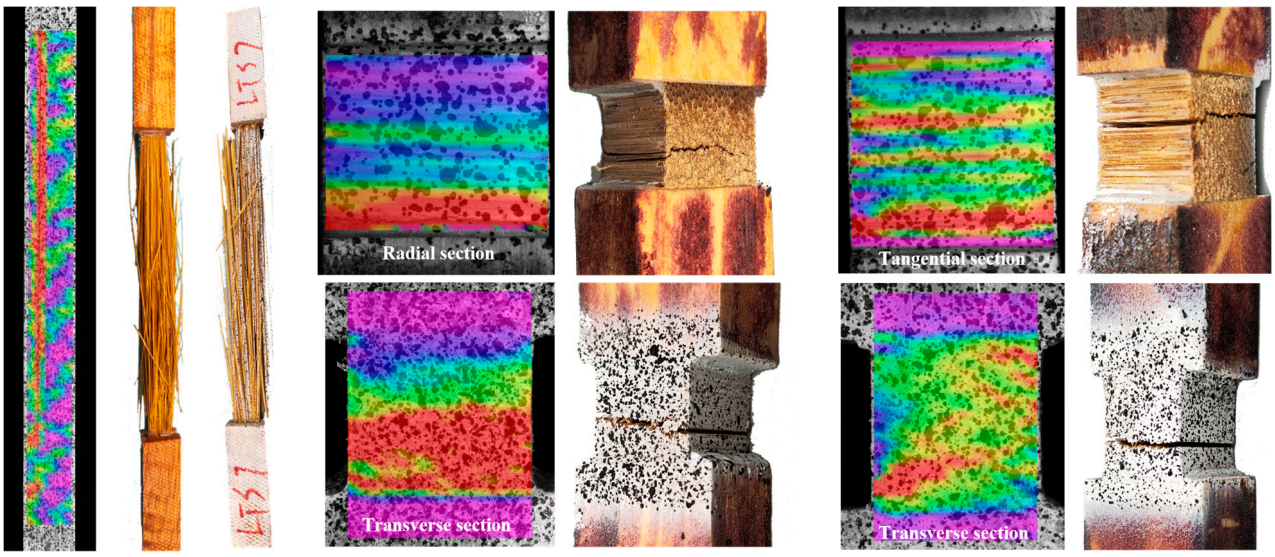

Figure 4. Typical schematic diagram and ultimate strain diagram of tensile damage of YDS: (**a**) longitudinal tensile damage specimen (bamboo green layer), (**b**) radial tensile damage specimen, (**c**) chordal tensile damage specimen.

3.1.2. Compression

As can be observed from the compression load-displacement curves presented in Figure 5, the longitudinal, radial and tangential compression of YDS displays clear elastic and elastoplastic behaviors [33]. With regard to longitudinal compression, as illustrated in Figure 5a, upon reaching the ultimate load, the curve declines gradually until failure. The average maximum load of longitudinal compression is observed to be as high as 18,501 N, which is approximately five times the average maximum load of chordal compression (3745 N). The radial and tangential compression curves exhibit a resemblance to those illustrated in Figure 5b,c, with the primary distinction being that the maximum load does not occur in radial compression. This is due to the fact that the density of the green side of YDS decreases towards the yellow side. Consequently, the bamboo material will undergo gradual compression and compaction during the radial compression process.

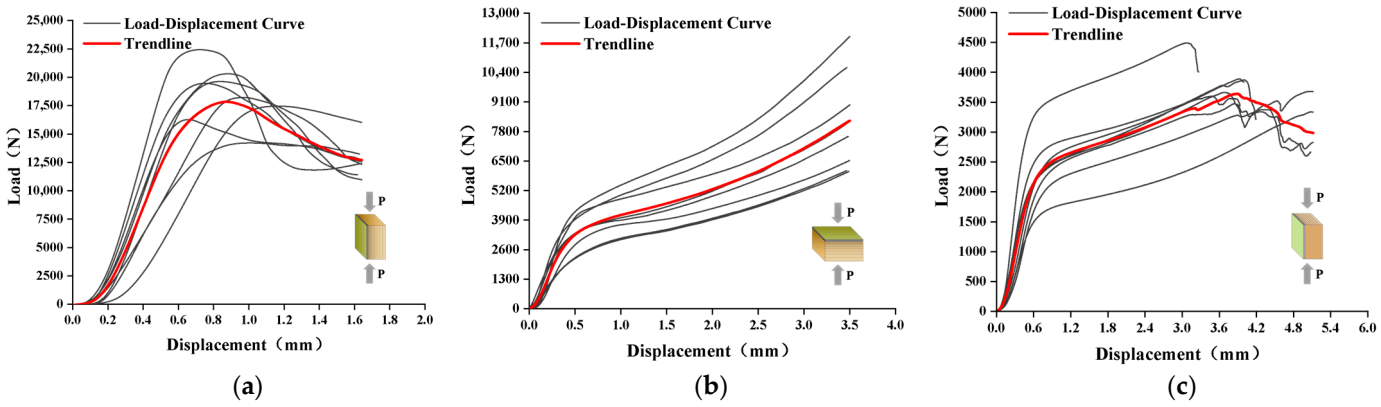

Figure 5. Compression load-displacement curves of YDS: (**a**) longitudinal compression, (**b**) radial compression, (**c**) tangential compression.

As illustrated in the schematic of typical compression damage and the ultimate strain map of Figure 6, during the longitudinal compression of YDS, the bamboo material initially displays distinct compressive creasing in the region of the bamboo yellow coloring, with no apparent damage evident in the region closer to the bamboo green. Furthermore, a shear damage trace of approximately 45° gradually emerges at the end of the radial section, originating from the side in proximity to the bamboo green and progressively extending towards the bamboo yellow region, as illustrated in Figure 6a. The tangential compression damage of bamboo is primarily evident in the compaction failure observed near the bamboo green side. Conversely, the bamboo yellow side exhibits no discernible damage traces, as illustrated in Figure 6b. The radial compression of bamboo consistently exhibited no discernible evidence of damage. However, the bamboo yellow region demonstrated a gradual compaction under the increasing load, a phenomenon more readily discernible in the strain diagram depicted in Figure 6c.

3.1.3. Shear

In the YDS shear test, it was observed that the radial direction of the bamboo exhibited greater resistance to shear loads than the tangential direction. The radial shear of the bamboo demonstrated a shear load capacity of approximately 1259 N, while the tangential shear exhibited a load capacity of approximately 784 N. From the curves, it can be observed that the radial shear damage mode of YDS exhibits brittle damage, as illustrated in Figure 7a. Conversely, the tangential shear demonstrates brittle damage following a brief load retention period after reaching the ultimate load, as depicted in Figure 7b. The radial and tangential shear damage of YDS is analogous in that it occurs at the stress concentration in the shear surface, as illustrated in Figure 7c,d.

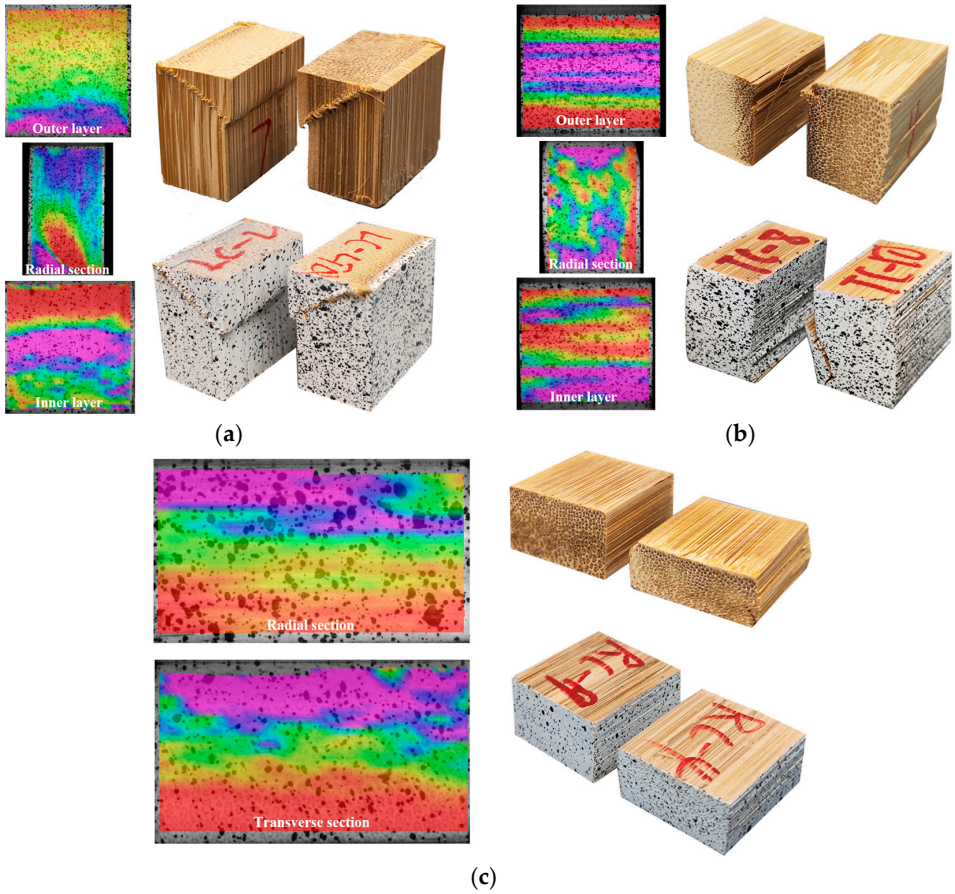

Figure 6. Typical damage schematic and ultimate strain diagram of YDS in compression: (**a**) longitudinal compression, (**b**) tangential compression, (**c**) radial compression.

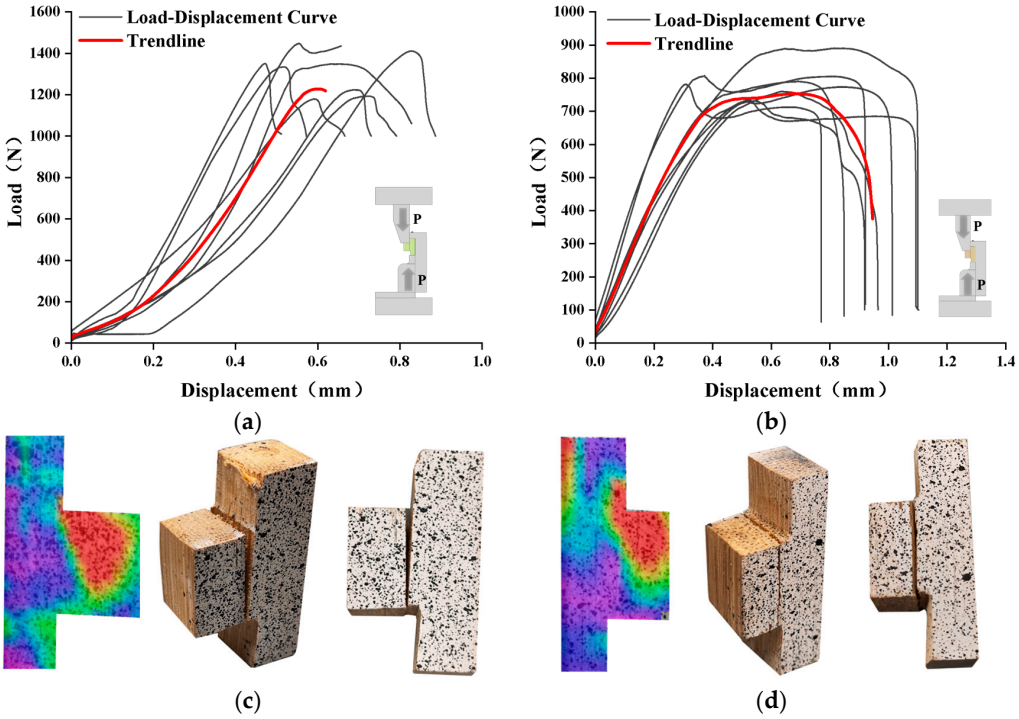

Figure 7. Radial and tangential shear load-displacement curves and damage typical diagrams and ultimate strain diagrams of YDS: (**a**,**c**) radial shear, (**b**,**d**) tangential shear.

3.2. Stress-Strain Analysis

3.2.1. Tensile Stress-Strain

In the longitudinal tensile test, the density and fiber bundles of YDS decrease from the green to the yellow stage [34], which results in a significant discrepancy in the strains observed on either side of the bamboo, with the same load applied, due to the aforementioned changes. The DIC expansion technique was employed to analyze the stress-strain behavior in the chordal plane of the bamboo green layer, the bamboo flesh layer, and the bamboo yellow layer of the bamboo material. Additionally, the change in stress-strain of the bamboo material, including the bamboo green, the bamboo flesh, and the bamboo yellow, was investigated on the radial plane.

In the longitudinal tensile test, the trends of the stress-strain curves were similar overall, with the exception of the bamboo green layer, which exhibited a distinctive stress-strain curve. In the case of the bamboo green layer, the longitudinal strain exceeded the tangential strain during the elastic phase. Conversely, the longitudinal strain exhibited minimal change in response to stress during the strengthening phase. In contrast, the tangential strain increased markedly, as illustrated in Figure 8a. The maximum tangential strain (−1.558%) was approximately 1.5 times the maximum longitudinal strain (0.964%). The stress-strain curves of bamboo flesh and bamboo yellow exhibit a high degree of similarity, as illustrated in Figure 8b,c. The maximum longitudinal strains observed were 1.308% and 1.465%, while the maximum tangential strains reached −0.413% and −0.374%, respectively. In the case of bamboo timber comprising all three varieties (bamboo green, bamboo flesh, and bamboo yellow), the maximum longitudinal strain is 1.311% and the maximum radial strain is −0.260%. Therefore, from the test results, the longitudinal strain in the longitudinal tensile process of YDS from bamboo green to bamboo flesh to bamboo yellow was the largest in the bamboo yellow layer under the same stress state, indicating that the bamboo yellow layer is more susceptible to longitudinal deformation than the bamboo green layer and the bamboo flesh layer. This is because the density of fiber bundles in bamboo increases from bamboo yellow to bamboo green layer by layer in the radial direction, and the mechanical properties of each layer decrease from bamboo green layer to bamboo yellow layer [35].

The longitudinal and tangential strain distributions of bamboo green, bamboo flesh, and bamboo yellow at varying stages of elasticity indicate that the region of maximum strain initially manifested at the bamboo's edge and subsequently expanded towards the interior. Ultimately, the bamboo sustained damage at the region of maximum tangential. The longitudinal and radial strains of the bamboo timber containing bamboo green, bamboo flesh and bamboo yellow are relatively constant in the elastic phase. Furthermore, the maximum strain region, which is concentrated on the bamboo green side, expands with increasing stress.

The radial and tangential tensile strength of YDS was compromised at low stress (4–7 MPa), and the stress fluctuation range was considerable during the collection process. Consequently, the stress curves obtained were highly disordered. To analyze the strain of the bamboo under different states, the image state of DIC collection was employed as a representation of the stress state.

The longitudinal and tangential strains in the radial stretching process are minimal, approaching zero. This is due to the fact that the maximum strain region of bamboo is primarily concentrated in the region adjacent to the yellow side of the bamboo, and the longitudinal and tangential strains in the region of bamboo damage are also very small. The longitudinal and tangential strains are relatively constant, whereas the radial strains are evident from the outset of the strain field stratification phenomenon, with the maximum radial strains concentrated in the region proximate to the yellow side of the bamboo, as illustrated in Figure 9.

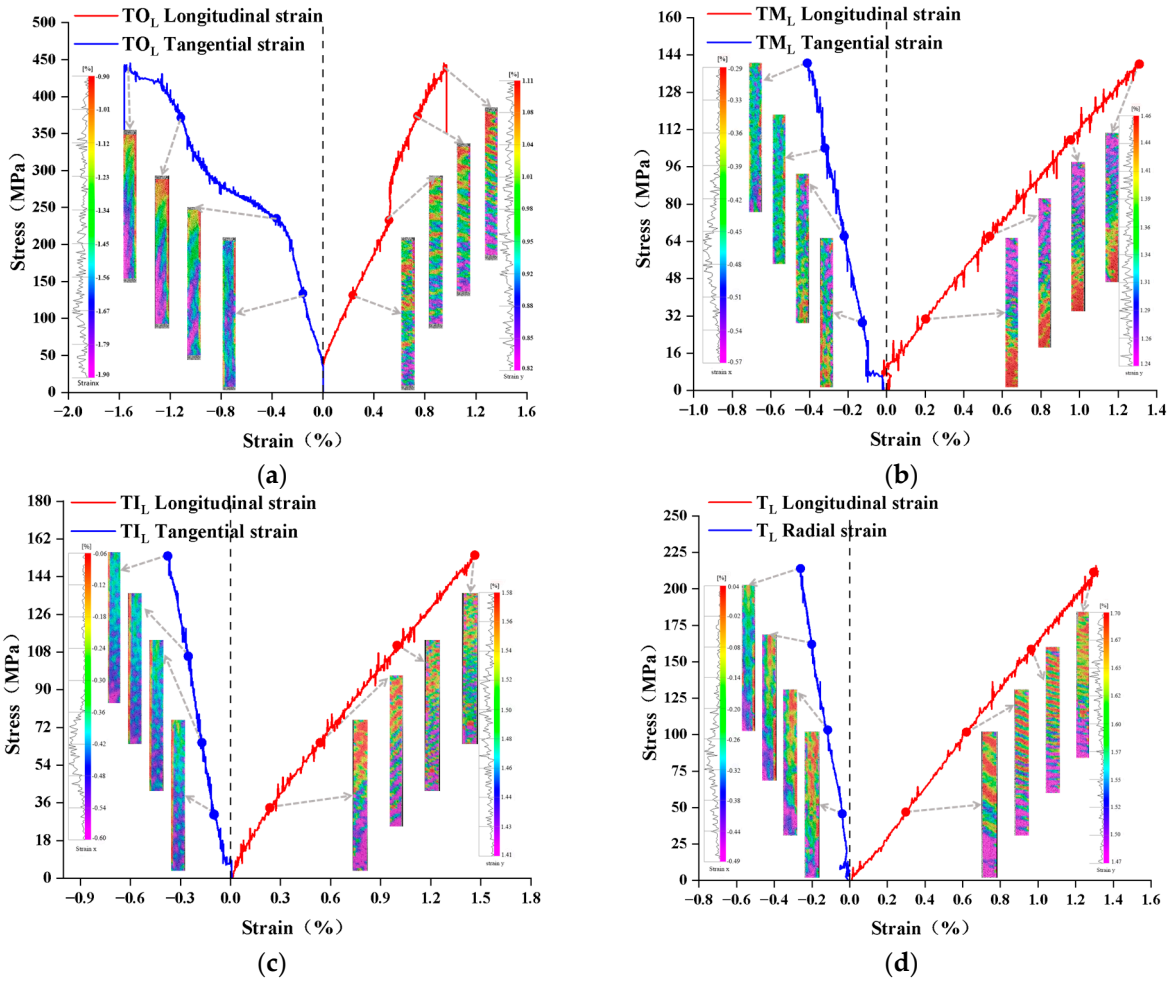

Figure 8. Longitudinal tensile stress-strain of YDS: (**a**) stress-strain of bamboo green layer (*LT*), (**b**) stress-strain of bamboo flesh layer (*LT*), (**c**) stress-strain of bamboo yellow layer (*LT*), and (**d**) stress-strain of the layer containing bamboo green, flesh, and yellow (*LR*). The gray dashed line in the figure represents the strain zero line, and subsequent representations will be the same.

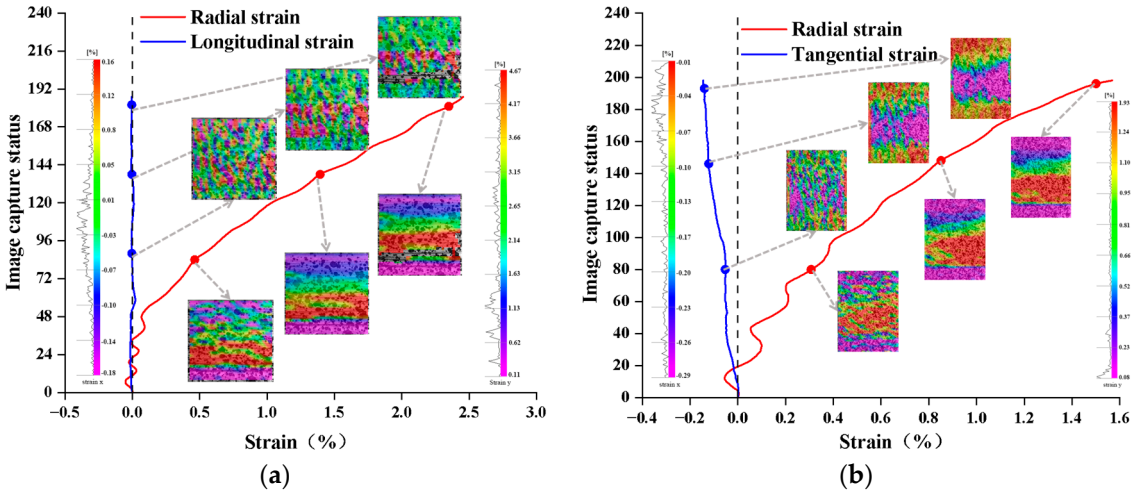

Figure 9. Radial tensile stress-strain of YDS: (**a**) radial section (*RL*), (**b**) transverse section (*RT*).

During the tangential stretching process of bamboo, the longitudinal and radial strains exhibited minimal fluctuations, with the maximum tangential strain reaching approximately 1%. From the strain maps at different stages, it can be observed that the longitudinal

and radial strains remain relatively constant. The maximum tangential strain initially manifests on the side of bamboo designated as yellow and subsequently extends to the side of bamboo designated as green, as illustrated in Figure 10. This is since the density of the bamboo cross section decreases from bamboo green (0.811 g/cm^3) to bamboo yellow (0.523 g/cm^3), and the distribution of vascular bundles is different. The distribution of vascular bundles in the bamboo green layer was denser, so its density was higher, while the distribution of vascular bundles in the bamboo yellow layer was sparser, so its density was lower [36]. As a result, the bamboo green layer is better able to disperse and transfer stresses when subjected to loads, thus reducing the occurrence of localized stresses. On the other hand, the lower density of the yellow bamboo layer makes it easier to deform under stress, resulting in a significant increase in strain. As a result, the yellow side of the bamboo will experience greater strain than the green side of the bamboo in the chordwise tension process.

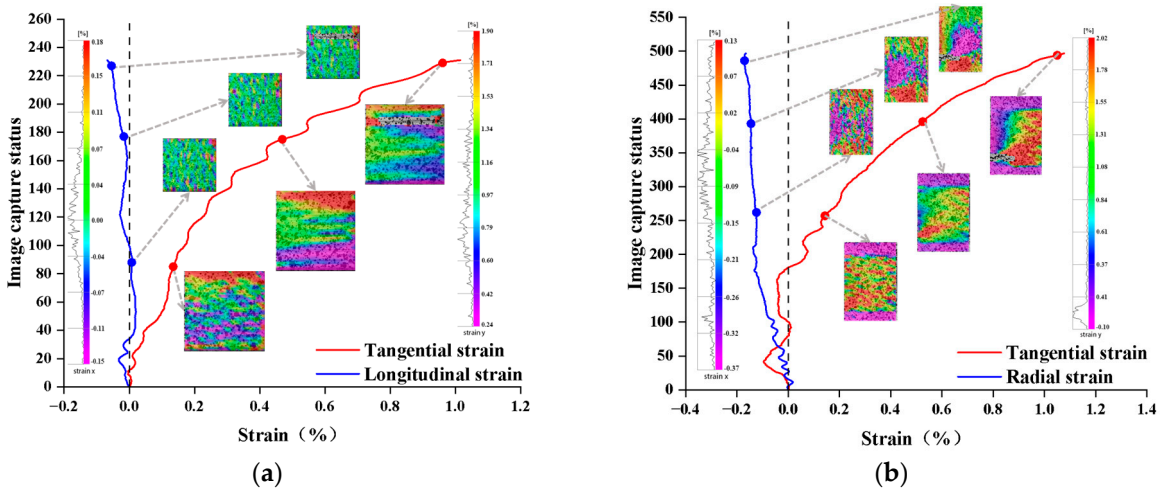

Figure 10. YDS chordal tensile stress-strain: (**a**) tangential section (*TL*), (**b**) transverse section (*TR*).

3.2.2. Compressive Stress-Strain

Upon reaching the ultimate stress, the maximum longitudinal strains on the bamboo green side, bamboo yellow side, and radial section were observed to be −0.718%, −1.414%, and −0.673%, respectively. The maximum tangential strains on the bamboo green side and the bamboo yellow side were found to be 0. The maximum radial strain on the radial section was 0.218%, indicating that the strain near the bamboo yellow side is larger than that near the bamboo green side. The maximum values were 0.389% and 0.433%, respectively. As can be observed in Figure 11, the maximum strain distribution near the yellow side of the bamboo is markedly more significant than that of the other two surfaces. This indicates that under equal stress conditions, the inner layer of YDS is more prone to compression deformation than the outer layer. This leads to non-uniform stress distribution in the bamboo material during the longitudinal compression process, making it susceptible to compression wrinkling and failure near the inner layer side.

In the radial compression process, the radial strain will increase in conjunction with the rise in stress. The longitudinal strain is almost negligible, the tangential strain is minimal in the plasticize stage and increases gradually after entering the plastic stage. Concurrently, the stress will not reach a turning point, as illustrated in Figure 12. This phenomenon can be attributed to the fact that the radial compression direction of bamboo is perpendicular to the arrangement of bamboo fiber bundles. As the stress increases, the bamboo material undergoes a gradual compaction process, changing from bamboo yellow to bamboo green. This results in the maximum stress-strain turning point not occurring. This is evident from the strain distribution diagrams on the radial and transverse sections, which illustrate that the radial and tangential strain distribution of bamboo is the most significant. The strain in the

region leaning into the bamboo yellow region is notably larger than that close to the bamboo green region. With the increase of stress, the maximum longitudinal strain distribution region is primarily concentrated in the region close to the bamboo yellow region.

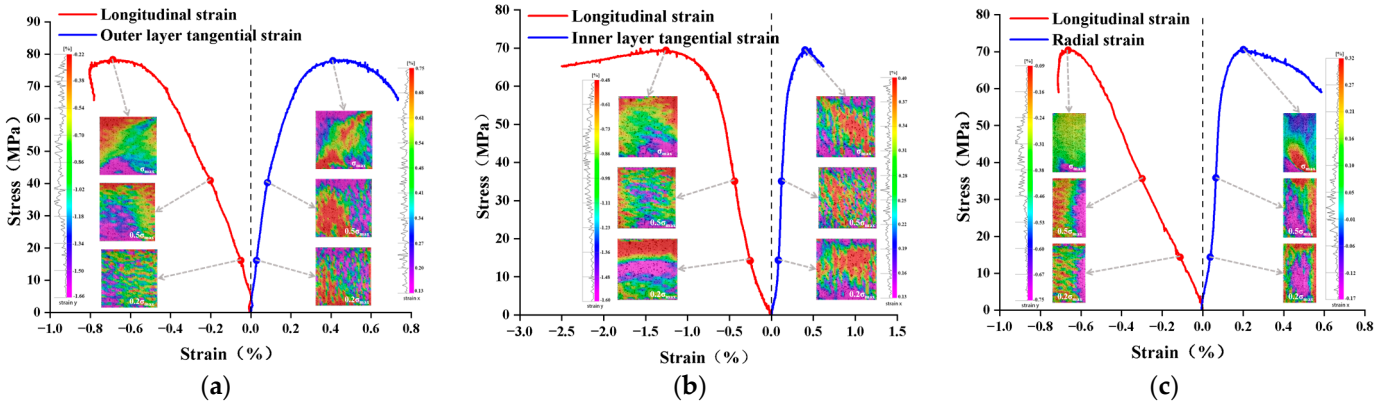

Figure 11. Longitudinal compressive stress-strain of YDS: (**a**) bamboo green tangential section (*LTO*) stress-strain, (**b**) bamboo yellow tangential section *(LTI*) stress-strain, (**c**) radial section (*LR*) stress-strain.

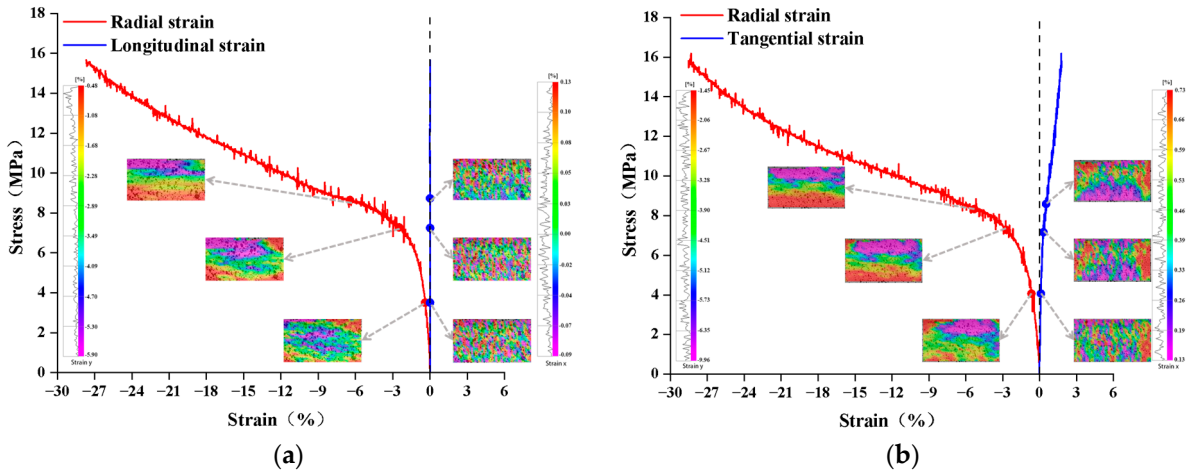

Figure 12. Radial compressive stress-strain of YDS: (**a**) radial section (RL) stress-strain, (**b**) transverse section (RT) stress-strain.

As illustrated in Figure 13, the stress-strain curves of YDS in tangential compression exhibit greater similarity to those in radial compression. The distinction between the two lies in the fact that tangential compression exhibits a turning point in stress reduction after sustained loading. Additionally, the longitudinal and radial strains are markedly minimal, while the radial strains demonstrate a gradual increase only when evidence of damage becomes apparent. In conditions of equivalent stress, the strain on the bamboo exhibiting yellow characteristics is still greater than that observed on the bamboo displaying green characteristics. This results in an eccentric force during the tangential compression process, causing the bamboo material to shift towards the yellow side and ultimately leading to cracking and destruction on the green side.

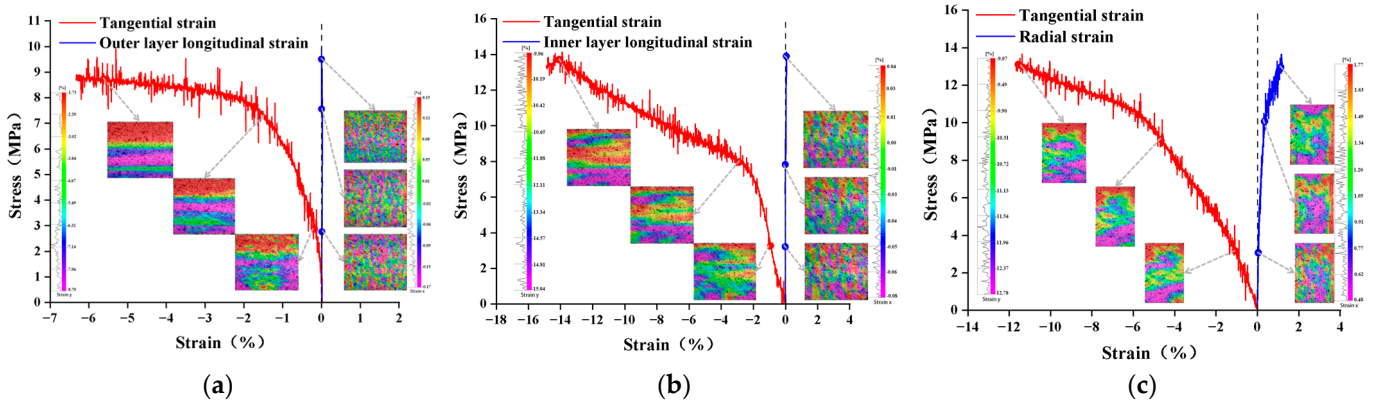

Figure 13. Tangential compressive stress-strain of YDS: (**a**) tangential section of bamboo green layer (TLO), (**b**) tangential section of bamboo yellow inner layer (TLI), (**c**) radial section (TR).

3.3. Strengths and Elastic Constants

3.3.1. Strengths

The maximum forces (F_{max}) and strengths (f) of the tensile, compression and shear of YDS are listed in Table 2, and the box plots of the tensile, compression, and shear strengths of YDS are given in Figure 14. It is evident that the longitudinal strength of YDS is the greatest in both tensile and compression. The longitudinal tensile strength is approximately four times that of the compression strength, which are 290.9 MPa and 77.1 MPa, respectively. The longitudinal tensile strength of the bamboo green layer was the highest at 378.8 MPa, which was significantly greater than that of the bamboo flesh layer (231.3 MPa) and the bamboo yellow layer (160.2 MPa), which was also exceeded the yield strength (355 MPa) of 45# steel [37], making it a potential high-strength engineering material or fiber-reinforced material.

Table 2. Maximum loads and strengths of YDS in tension, compression, and shear.

Type of Test		Tension						Compression		Shear	
		TO, L	TM, L	TI, L	T, L	T, R	T, T	C, L	C, T	S, R	S, T
F_{max} [N]	Avg	9850	7401	5125	7564	728	703	18,501	3745	1259	784
	SD	1502	1301	918	640	91	116	2548	357	126	51
	COV (%)	15.3	17.6	17.9	8.5	12.5	16.4	13.8	9.5	10	6.5
f [MPa]	Avg	378.8	231.3	160.2	290.9	5.1	4.9	77.1	14.9	7.1	4.4
	SD	57.8	40.6	28.7	24.6	0.6	0.8	10.6	1.4	0.7	0.3
	COV (%)	15.3	17.6	17.9	8.5	12.5	16.3	13.8	9.5	10	6.5

The longitudinal tensile strength of bamboo timber that contained the bamboo green, bamboo flesh, and bamboo yellow layer was intermediate between that of the bamboo green and bamboo flesh. The radial and tangential tensile, tangential compression, and radial and tangential shear strengths were all found to be extremely low, with a range of only 5 MPa to 15 MPa, which is not a significant difference. It was not possible to obtain the radial compression strength due to the specific nature of this test, which indicates that bamboo, as a naturally orthotropic material, exhibits excellent mechanical properties in the longitudinal direction, while being significantly weaker in the radial and tangential directions.

3.3.2. Modulus of Elasticity

The tensile and compressive modulus of elasticity (E) and shear modulus (G) are presented in Table 3, and the box plots of tensile and compressive modulus of elasticity and shear modulus of YDS are provided in Figure 15. As can be seen from Table 3 and Figure 15, the longitudinal tensile modulus of elasticity for YDS with a bamboo green layer is the highest at 30,805 MPa. This has reached the range of tensile elastic modulus values for the vascular bundles of bamboo (25–52 GPa) [38]. The second highest is that of

the bamboo flesh, as well as that of the bamboo containing bamboo green, bamboo flesh, and bamboo yellow, which are 16,547 MPa and 20,111 MPa, respectively. The modulus of elasticity of YDS in the longitudinal direction exhibited the highest values for both tensile and compressive loading, with a tensile modulus of elasticity approximately 50% higher than that observed in compression (16,771 MPa). The tensile, compressive and shear modulus of elasticity in the radial and tangential directions exhibited the lowest values, ranging from approximately 200 MPa to 500 MPa.

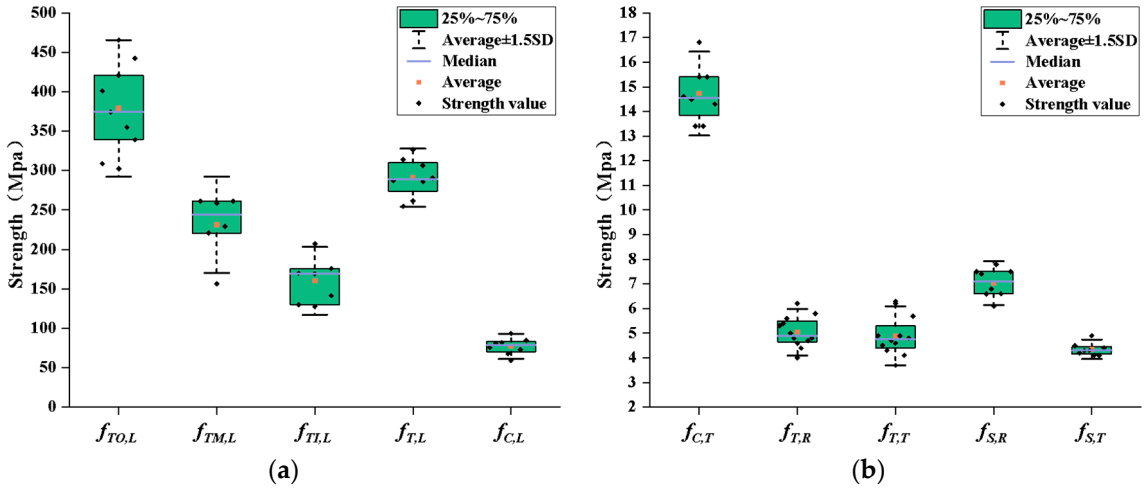

Figure 14. YDS tensile, compression and shear strength: (**a**) longitudinal tensile and longitudinal compression strength box plot, (**b**) radial and tangential tensile, tangential compression, radial and tangential shear strength box plot.

Table 3. Tensile and compressive modulus of elasticity *E* and shear modulus *G* of YDS.

Type of Test		TO, L	TM, L	TI, L	T, L	T, R	T, T	C, R	C, T	S, R	S, T
E (*G*) [MPa]	Avg	30,805	16,547	11,851	20,111	191	299	494	567	202	149
	SD	4860	3255	2374	2003	44	55	119	137	36	39
	COV (%)	15.7	19.7	20	10	23.1	18.4	23.9	24.1	17.9	26.2

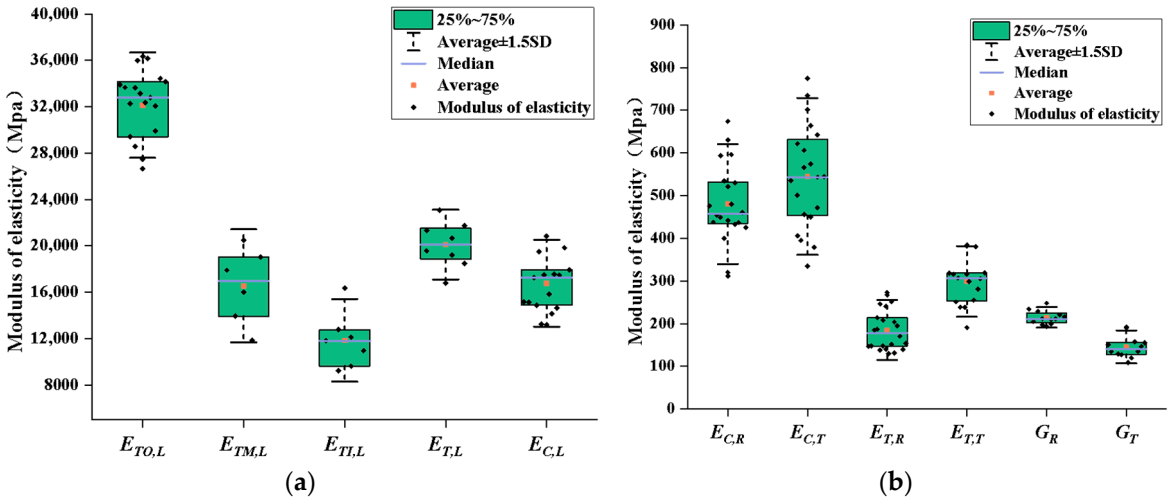

Figure 15. Tensile and compressive modulus of elasticity and shear modulus of YDS: (**a**) longitudinal tensile and compressive modulus of elasticity box plot, (**b**) radial and tangential tensile and compressive modulus of elasticity and shear modulus box plot.

3.3.3. Poisson's Ratio

The tensile and compressive Poisson's ratios μ_{LR}, μ_{LT}, μ_{RL}, μ_{RT}, μ_{TL}, and μ_{TR} of YDS are presented in Table 4. Additionally, the box line plots of the Poisson's ratios under tensile and compressive loading of YDS are provided in Figure 16. Table 4 and Figure 16 demonstrate that the μ_{LT} and μ_{LR} values exhibited the greatest Poisson's ratio in both longitudinal tension and compression. The μ_{LT} and μ_{LR} values were the highest for the bamboo green layer (0.512) and μ_{LTM} (0.343). Notably, the Poisson's ratio for bamboo green, bamboo flesh, and bamboo yellow exhibited the greatest magnitude. The Poisson's ratio μ_{LTO} (0.512) exhibited the greatest magnitude, while the Poisson's ratio μ_{LTM} (0.343) was observed in the bamboo flesh layer and the Poisson's ratio μ_{LR} (0.344). The Poisson's ratio μ_{LTI} (0.306) for the bamboo yellow layer was the smallest, as illustrated in Figure 16a. During longitudinal compression, the largest Poisson's ratio was μ_{LR} (0.422), followed by μ_{LTO} (0.299) for the bamboo green layer and μ_{LTI} (0.151) for the bamboo yellow layer, which exhibited the smallest value. This is illustrated in Figure 16c. It can be observed that the Poisson's ratio of YDS exhibits a gradual decrease from the bamboo green layer to the bamboo yellow layer. This is consistent with the research findings of Lu et al. [22]. This trend is also evident in the chordal compression process, with the Poisson's ratio μ_{TLO} (0.020) near the bamboo green layer being larger than that μ_{TLI} (0.005) near the bamboo yellow layer (Figure 16d). From the histograms of tensile and compressive Poisson's ratios of YDS, it can be observed that the discrepancy between tensile and compressive Poisson's ratios in the radial and chordal directions is not significant, with all values remaining relatively low. However, the divergence between tensile and compressive Poisson's ratios in the longitudinal direction is notable, as illustrated in Figure 16e.

Table 4. Poisson's ratios of YDS in tensile and compressive stress states.

Type of Test		μ_{LR}	μ_{LTO}	μ_{LTM}	μ_{LTI}	μ_{RL}	μ_{RT}	μ_{TLO}	μ_{TLI}	μ_{TR}
Tension	Avg	0.344	0.512	0.343	0.306	0.024	0.156	0.029	-	0.102
	SD	0.073	0.071	0.059	0.062	0.008	0.047	0.008	-	0.034
	COV (%)	21.1	13.8	17.1	20.4	32.9	29.9	28.3	-	32.8
Compression	Avg	0.422	0.299	-	0.151	0.018	0.147	0.020	0.005	0.179
	SD	0.083	0.057	-	0.033	0.006	0.027	0.004	0.002	0.063
	COV (%)	19.7	19.0	-	21.7	33.8	18.7	21.8	37.8	20.1

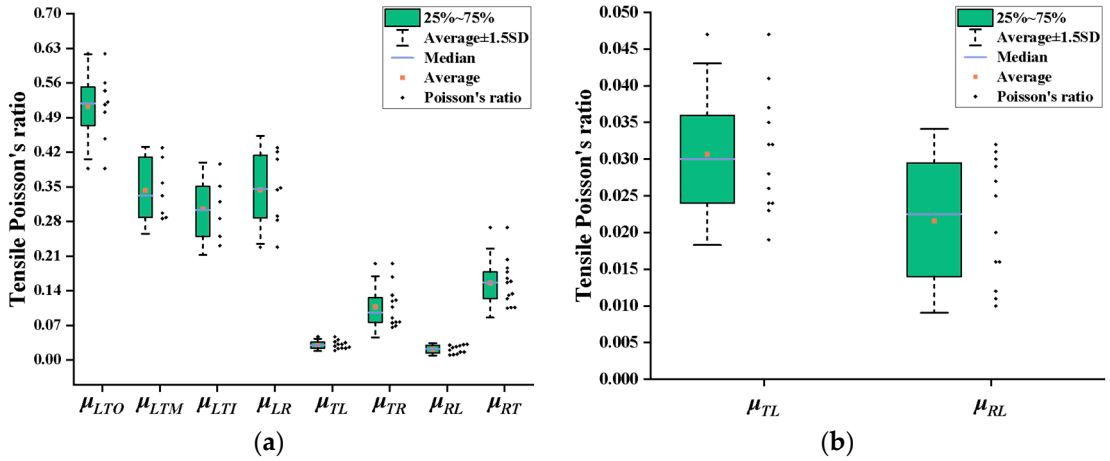

Figure 16. *Cont.*

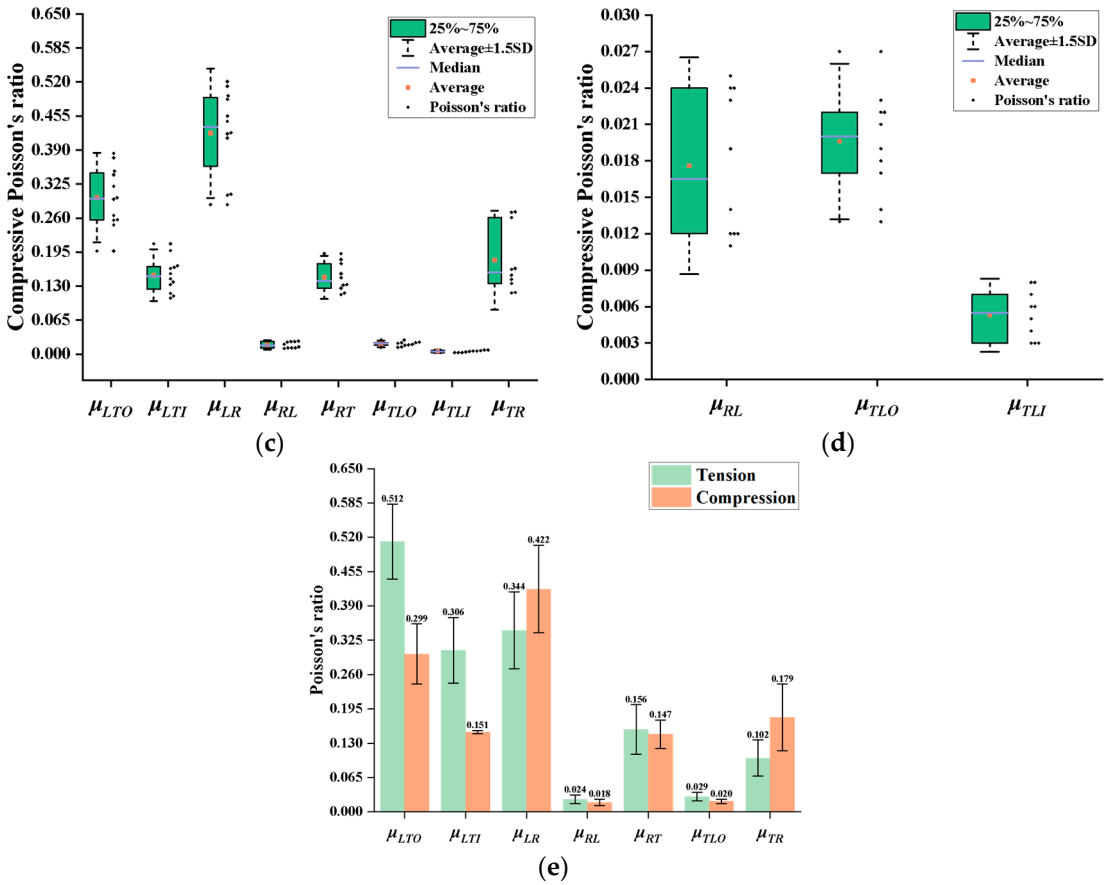

Figure 16. Tensile and compressive Poisson's ratios of YDS: (**a**) box line plot of Poisson's ratio under tensile loading, (**b**) local magnification of μ_{TL} and μ_{RL} in (**a**), (**c**) box line plot of Poisson's ratio under compressive loading, (**d**) local magnification of μ_{TLO}, μ_{TLI}, and μ_{RL} in (**c**), (**e**) comparative histogram of Poisson's ratio under tensile and compressive Poisson's ratio comparison histograms under loading.

4. Conclusions

This paper presents the findings of an investigation into the basic mechanical properties and elastic constants of small specimens of YDS. The main conclusions are as follows:

(1) The gradient longitudinal tensile mechanical properties of YDS, from the bamboo green to the bamboo yellow layers, were determined. The bamboo green layer exhibited the highest longitudinal tensile properties, followed by the bamboo flesh layer, with the bamboo yellow layer showing the lowest. The longitudinal tensile strength of the bamboo green layer, denoted as $f_{TO,L}$, was found to be 40% and 136% greater than that of the bamboo flesh layer, $f_{TM,L}$, and the bamboo yellow layer, $f_{TI,L}$, respectively. Similarly, the longitudinal tensile modulus of elasticity of the bamboo green layer, $E_{TO,L}$, was 86% and 160% higher than that of the bamboo flesh layer, $E_{TM,L}$, and the bamboo yellow layer, $E_{TI,L}$, respectively.

(2) YDS exhibits significant anisotropy, with its longitudinal properties (including the green, flesh, and yellow layers) being the most superior in terms of strength and elastic modulus. The longitudinal tensile strength ($f_{T,L}$) and compressive strength ($f_{C,L}$) reach up to 290 MPa and 77 MPa, respectively; the longitudinal tensile modulus (ET,L) and compressive modulus ($E_{C,L}$) attain values of 20,111 MPa and 16,771 MPa, respectively. In contrast, the radial and tangential properties are relatively inferior, with tensile strength ($f_{T,R}$, $f_{T,T}$), compressive strength ($f_{C,T}$), and shear strength ($f_{S,R}$, $f_{S,T}$) only ranging from approximately 5 to 15 MPa; the radial and tangential tensile

modulus ($E_{T,R}$, $E_{T,T}$), compressive modulus ($E_{C,R}$, $E_{C,T}$), and shear modulus (G_R, G_T) are only in the range of approximately 200 to 500 MPa.

(3) The Poisson's ratios of YDS under tensile stress are μ_{LTO} = 0.512, μ_{LTM} = 0.343, μ_{LTI} = 0.306, μ_{LR} = 0.344, μ_{RL} = 0.024, μ_{RT} = 0.156, μ_{TLO} = 0.029, and μ_{TR} = 0.102, and under compressive stress are μ_{LR} = 0.422, μ_{RL} = 0.018, μ_{RT} = 0.147, μ_{TR} = 0.179, μ_{LTO} = 0.299, μ_{LTI} = 0.151, μ_{TLO} = 0.020, and μ_{TLI} = 0.005.

(4) This study comprehensively investigated the fundamental mechanical properties and elastic constants of bamboo, particularly through systematic testing of the variation in elastic modulus and Poisson's ratio from the green to the yellow layers of YDS. This not only compensates for the deficiencies in previous research but also provides essential foundational data and theoretical support for predicting the mechanical behavior and numerical simulation of bamboo in structural applications. These findings can more accurately inform the design and assessment of bamboo structures, promoting the use of bamboo as a renewable and environmentally friendly material in the fields of construction and engineering.

Author Contributions: Conceptualization, C.D.; Software, Y.W.; Formal analysis, F.Z.; Data curation, F.Z., X.W. and G.L.; Writing—original draft, F.Z.; Visualization, F.Z.; Supervision, C.D.; Project administration, C.D.; Funding acquisition, C.D. All authors have read and agreed to the published version of the manuscript.

Funding: This work was supported by the National Natural Science Foundation of China (No. 31960291). Yunnan Agricultural Joint Specialization (No. 202301BD070001-060). Yunnan Provincial Reserve Program for Young and Middle-aged Academic and Technical Leaders (No. 202305AC160074).

Data Availability Statement: Data are contained within the article.

Conflicts of Interest: The authors declare no conflict of interest.

References

1. Huang, X.H. Studies on the Reproduction of *Dendroncalamus sinicus*. Master's Thesis, Southwest Forestry College, Kunming, China, 2008.
2. Liu, R.H.; Cheng, D.R.; Shi, Z.J.; Liu, W.Y.; Hui, C.M.; Deng, J. Study on Physical Properties of Thin-Culm-Wall *Dendrocalamus sinicus*. *World Bamboo Ratt. Newsl.* **2015**, *13*, 14–17. [CrossRef]
3. Liu, S.N.; Hui, C.M. Research Status and Outlook of Rare Bamboo Species of *Dendrocalamus sinicus*. *World Bamboo Ratt. Newsl.* **2011**, *9*, 26–30. [CrossRef]
4. Li, P.J. Research on the Tectonics of Raw Bamboo Architecture: Taking Yunnan *Dendrocalamus sinicus* as an Example. Master's Thesis, Kunming University of Science and Technology, Kunming, China, 2022. [CrossRef]
5. Ma, Y.F.; Luan, Y.; Chen, L.; Huang, B.; Luo, X.; Miao, H.; Fang, C.H. A Novel Bamboo–Wood Composite Utilizing High-Utilization, Easy-to-Manufacture Bamboo Units: Optimization of Mechanical Properties and Bonding Performance. *Forests* **2024**, *15*, 716. [CrossRef]
6. Zhang, X.B.; Jiang, Z.H.; Fei, B.H.; Fang, C.H.; Liu, H.R. Experimental performance of threaded steel glued into laminated bamboo. *Constr. Build. Mater.* **2020**, *249*, 118780. [CrossRef]
7. Almeida, A.C.D.; Araujo, V.A.D.; Morales, E.A.M.; Gava, M.; Munis, R.A.; Garcia, J.N.; Cortez-Barbosa, J. Wood-bamboo particleboard: Mechanical properties. *BioResources* **2017**, *12*, 7784–7792. [CrossRef]
8. Chen, M.L.; Semple, K.; Hu, Y.A.; Zhang, J.L.; Zhou, C.L.; Pineda, H.; Xia, Y.L.; Zhu, W.K.; Dai, C.P. Fundamentals of Bamboo Scrimber Hot Pressing: Mat Compaction and Heat Transfer Process. *Constr. Build. Mater.* **2024**, *412*, 134843. [CrossRef]
9. Wang, F.L.; Shao, Z.P. Study on the Variation Law of Bamboo Fibers' Tensile Properties and the Organization Structure on the Radial Direction of Bamboo Stem. *Ind. Crops Prod.* **2020**, *152*, 112521. [CrossRef]
10. Liu, P.C.; Zhou, Q.S.; Zhang, H.; Tian, J.F. Experimental Research on the Compressive Performance of Raw Bamboo Materials along the Grain. *J. Phys. Conf. Ser.* **2021**, *1798*, 012004. [CrossRef]
11. Krause, J.Q.; De Andrade Silva, F.; Ghavami, K.; Gomes, O.D.F.M.; Filho, R.D.T. On the Influence of Dendrocalamus Giganteus Bamboo Microstructure on Its Mechanical Behavior. *Constr. Build. Mater.* **2016**, *127*, 199–209. [CrossRef]
12. Huang, X.Y.; Xie, J.L.; Qi, J.Q.; De Hoop, C.F.; Xiao, H.; Chen, Y.Z.; Li, F. Differences in physical–mechanical properties of bamboo scrimbers with response to bamboo maturing process. *Eur. J. Wood Wood Prod.* **2018**, *76*, 1137–1143. [CrossRef]
13. Wang, Z.W.; Zhang, X.W.; Yao, L.H.; Zhang, Q.M. Experimental study and numerical simulation on the macro and micro mechanical properties of bamboo. *J. For. Eng.* **2022**, *7*, 31–37. [CrossRef]
14. Yang, T.C.; Yang, H.Y. Strain analysis of Moso bamboo (*Phyllostachys pubescens*) subjected to longitudinal tensile force. *Mater. Today Commun.* **2021**, *28*, 102491. [CrossRef]

15. Sharma, B.; Harries, K.A.; Ghavami, K. Methods of determining transverse mechanical properties of full-culm bamboo. *Constr. Build. Mater.* **2013**, *38*, 627–637. [CrossRef]
16. Zhou, Q.S.; Tian, J.F.; Liu, P.C.; Zhang, H. Test and Prediction of Mechanical Properties of Moso Bamboo. *J. Eng. Fibers Fabr.* **2021**, *16*, 155892502110668. [CrossRef]
17. Tinkler-Davies, B.; Shah, D.U. Digital Image Correlation Analysis of Laminated Bamboo under Transverse Compression. *Mater. Lett.* **2021**, *283*, 128883. [CrossRef]
18. Liu, P.C.; Zhou, Q.S.; Zhang, H.; Tian, J.F. Design Strengths of Bamboo Based on Reliability Analysis. *Wood Mater. Sci. Eng.* **2023**, *18*, 222–232. [CrossRef]
19. Sandhaas, C.; Sarnaghi, A.K.; van de Kuilen, J.W. Numerical modelling of timber and timber joints: Computational aspects. *Wood Sci. Technol.* **2020**, *54*, 31–61. [CrossRef]
20. Gilbert, B.P.; Bailleres, H.; Zhang, H.; McGavin, R.L. Strength Modelling of Laminated Veneer Lumber (LVL) Beams. *Constr. Build. Mater.* **2017**, *149*, 763–777. [CrossRef]
21. Molari, L.; Coppolino, F.S.; García, J.J. Arundo donax: A widespread plant with great potential as sustainable structural material. *Constr. Build. Mater.* **2021**, *268*, 121143. [CrossRef]
22. Lu, H.J.; Lian, H.Y.; Xu, J.Y.; Ma, N.N.; Zhou, Z.Z.; Song, Y.P.; Yu, Y.M.; Zhang, X.C. Study on the Variation Pattern and Influencing Factors of Poisson's Ratio of Bamboo. *Front. Mater.* **2022**, *9*, 896756. [CrossRef]
23. García, J.J.; Rangel, C.; Ghavami, K. Experiments with rings to determine the anisotropic elastic constants of bamboo. *Constr. Build. Mater.* **2012**, *31*, 52–57. [CrossRef]
24. Dixon, P.G.; Gibson, L.J. The structure and mechanics of Moso bamboo material. *J. R. Soc. Interface* **2014**, *11*, 20140321. [CrossRef] [PubMed]
25. *D07 Committee*; Test Methods for Small Clear Specimens of Timber. ASTM International: West Conshohocken, PA, USA, 2014. [CrossRef]
26. *JG/T 199-2007*; Test Method for Physical and Mechanical Properties of Bamboo for Construction. Ministry of Construction of the People's Republic of China: Beijing, China, 2007.
27. Wang, J.F.; Lu, C.F.; Tian, E.B.; Wang, H.Y. Experimental Research on the Mechanical Properties of Sanming *Phyllostachys pubescen* Along the Grain Direction. *J. Sanming Univ.* **2021**, *38*, 93–101. [CrossRef]
28. Tan, T.; Rahbar, N.; Allameh, S.M.; Kwofie, S.; Dissmore, D.; Ghvami, K.; Soboyejo, W.O. Mechanical properties of functionally graded hierarchical bamboo structures. *Acta Biomater.* **2011**, *7*, 3796–3803. [CrossRef] [PubMed]
29. Liu, H.R.; Jiang, Z.H.; Fei, B.H.; Hse, C.Y.; Sun, Z.J. Tensile behaviour and fracture mechanism of moso bamboo (*Phyllostachys pubescens*). *Holzforschung* **2015**, *69*, 47–52. [CrossRef]
30. Shao, Z.P.; Fang, C.H.; Huang, S.X.; Tian, G.L. Tensile properties of Moso bamboo (*Phyllostachys pubescens*) and its components with respect to its fiber-reinforced composite structure. *Wood Sci. Technol.* **2010**, *44*, 655–666. [CrossRef]
31. Cui, J.; Mi, L.; Li, L.; Liu, Y.; Wang, C.; He, C.; Zhang, H.; Chen, Y.; Wang, Q. Stepwise failure behavior of thermal-treated bamboo under uniaxial tensile load. *Ind. Crops Prod.* **2023**, *204*, 117313. [CrossRef]
32. Cai, X.F.; Wang, M.T.; Lu, Y.B.; Noori, A.; Chen, J.; Chen, F.M.; Chen, L.B.; Jing, X.Q.; Zhang, Q.H. Experimental study on the dynamic tensile failure of bamboo. *Constr. Build. Mater.* **2023**, *392*, 131886. [CrossRef]
33. Wang, M.T.; Cai, X.F.; Lu, Y.B.; Noori, A.; Chen, F.M.; Chen, L.B.; Jiang, X.Q. Mechanical behavior and failure modes of bamboo scrimber under quasi-static and dynamic compressive loads. *Eng. Fail. Anal.* **2023**, *146*, 107006. [CrossRef]
34. Tsuyama, T.; Hamai, K.; Kijidani, Y.; Sugiyama, J. Quantitative morphological transformation of vascular bundles in the culm of moso bamboo (*Phyllostachys pubescens*). *PLoS ONE* **2023**, *18*, e0290732. [CrossRef]
35. Gong, Z.H.; Zhang, W.; Zhou, C.; Yao, W.B.; Yu, W.P.; Zhang, T.Y. Examination of bamboo single layer linear tensile property. *J. For. Eng.* **2023**, *8*, 58–63. [CrossRef]
36. Li, H.B.; Zhu, Q.P.; Lu, P.C.; Chen, X.; Xian, Y. The Gradient Variation of Location Distribution, Cross-Section Area, and Mechanical Properties of Moso Bamboo Vascular Bundles along the Radial Direction. *Forests* **2024**, *15*, 1023. [CrossRef]
37. Chen, F.; Wang, X.D.; Shi, Y.G.; Zhang, Z.Y.; Wang, Z.K. Discussion on the Law of Mechanical Properties of 45 Steel. *Shanxi Metall.* **2021**, *44*, 89–90+93. [CrossRef]
38. An, X.J.; Wang, H.; Li, W.J.; Wang, H.K.; Yu, Y. Tensile mechanical properties of fiber sheaths microdissected from moso bamboo. *J. Nanjing For. Univ. (Nat. Sci. Ed.)* **2014**, *38*, 6–10. [CrossRef]